Andean Geology 52 (3): 363-382. September, 2025
doi: 10.5027/andgeoV52n3-3719

Andean Geology
www.andeangeology.cl

Interaction between groundwater and meteoric water determined by stable isotopes ($\delta^{18}O$, $\delta^{2}H$), radiogenic isotopes ($^{87}Sr/^{86}Sr$), and water chemistry: a case study from the Middle Magdalena Basin, Colombia

***Tania S. Palmera Henao[1], Mario García González[2], María I. Marín Cerón[1]**

[1] *Universidad EAFIT, Departamento de Ciencias de la Tierra, Escuela de Ciencias, Carrera 49 #7 sur 50, Medellín, Colombia. tspalmerah@eafit.edu.co, mmarince@eafit.edu.co*

[2] *Universidad Industrial de Santander, Facultad de Ingenierías Fisicoquímicas, Escuela de Geología, Calle 9 #27, Bucaramanga, Colombia. mgarciag@uis.edu.co*

* *Corresponding author: tspalmerah@eafit.edu.co*

ABSTRACT. In mature oil-producing basins, managing water resources presents challenges due to the potential of enhanced oil recovery (EOR) techniques to counteract reservoir depletion. The water sources in production systems, whether from naturally infiltrated meteoric water, connate formation water, or fluids derived from EOR, add complexities to the isotopic and geochemical signatures of groundwater in reservoir fluids. The present study reports new data on the isotopic and chemical composition of groundwater associated with Oligocene Mugrosa Formation reservoirs in the Middle Magdalena Basin (MMB), Colombia. This research integrates conventional hydrochemical parameters (pH, electrical conductivity, and major ion composition), stable isotope data ($\delta^{18}O$ and $\delta^{2}H$), and radiogenic isotope ratios ($^{87}Sr/^{86}Sr$). The water samples were collected from production wells with selective completions in operational levels (depths ranging from ~800 to 1,950 m) of the Mugrosa Formation across fields P1-P6, ensuring samples representative of the targeted reservoir intervals. These water samples are unaffected by EOR operations, thereby providing data that reflect the natural, undisturbed conditions of the reservoirs. Ionic and isotopic analyses indicate interaction between meteoric and connate waters within the MMB. Meteoric waters, which are chemically less evolved and isotopically depleted in $\delta^{18}O$ and $\delta^{2}H$, exhibit short relative residence times in the system and are primarily present along the eastern part of the basin, particularly in the eastern flank of the Nuevo Mundo Syncline. In contrast, connate waters are characterized by longer relative residence times, more evolved chemical compositions, and isotopic enrichment in $\delta^{18}O$ and $\delta^{2}H$. These latter samples are located on the western flank of the Peña de Oro Syncline and in proximity to the Arrugas and Casabe thrust faults. This study suggests that groundwater in the MMB originates from two primary sources: 1) infiltration of meteoric water, and 2) upward migration of deep saline waters derived from Cretaceous formations. Meteoric water infiltrates along the eastern basin margin and migrates through the Mugrosa Formation, where water-rock interactions progressively alter their chemical composition, most notably increasing sodium, calcium, and potassium concentrations. Connate waters from underlying Cretaceous formations ascend along reverse fault planes, mixing with meteoric waters and modifying their chemical and isotopic signatures. This mixing results in elevated chloride concentrations and an enrichment in $\delta^{18}O$ relative to local meteoric water values.

Keywords: Radiogenic isotopes ($^{87}Sr/^{86}Sr$), Stable isotopes ($\delta^{18}O$, $\delta^{2}H$), Water mixtures, Meteoric waters, Connate waters.

RESUMEN. Interacción entre aguas subterráneas y meteóricas determinadas por isótopos estables ($\delta^{18}O$, $\delta^{2}H$), isótopos radiogénicos ($^{87}Sr/^{86}Sr$) y química de aguas: un caso de estudio de la Cuenca del Magdalena Medio, Colombia. En cuencas maduras productoras de hidrocarburos, la gestión de los recursos hídricos presenta desafíos debido al potencial de las técnicas de recobro mejorado de petróleo (EOR, por sus siglas en ingles) para contrarrestar el agotamiento del yacimiento. Las fuentes de agua en los sistemas de producción, ya sean aguas meteóricas infiltradas de forma natural, aguas connatas de formación o fluidos derivados de procesos EOR, generan complejidades en las firmas isotópicas y geoquímicas de las aguas subterráneas presentes en los fluidos de reservorio. El presente estudio aporta nuevos datos sobre la composición isotópica y química de aguas subterráneas asociadas con los reservorios de la Formación Mugrosa (Oligoceno) en la Cuenca del Magdalena Medio (CMM), Colombia. Esta investigación integra parámetros hidroquímicos convencionales (pH, conductividad eléctrica y composición iónica mayoritaria), datos de isótopos estables ($\delta^{18}O$ y $\delta^{2}H$) y relaciones isotópicas radiogénicas ($^{87}Sr/^{86}Sr$). Las muestras de agua se recolectaron en pozos productores de la Formación Mugrosa a niveles operacionales (profundidades entre ~800 y 1.950 m). Estas muestras de agua no presentan influencia de procesos EOR, por lo que los datos obtenidos reflejan las condiciones naturales no perturbadas del reservorio. Los análisis iónicos e isotópicos indican interacción entre aguas meteóricas y connatas en la CMM. Las aguas meteóricas, químicamente menos evolucionadas y empobrecidas isotópicamente en $\delta^{18}O$ y $\delta^{2}H$, presentan tiempos de residencia en el sistema relativamente cortos y se localizan principalmente en el sector oriental de la cuenca, en particular en el flanco oriental del Sinclinal Nuevo Mundo. En contraste, las aguas connatas se caracterizan por mayores tiempos relativos de residencia, composiciones químicas más evolucionadas y enriquecimiento isotópico en $\delta^{18}O$ y $\delta^{2}H$. Estas últimas se ubican en el flanco occidental del Sinclinal Peña de Oro y en proximidad a las fallas de cabalgamiento de Arrugas y Casabe. Este estudio sugiere que el agua subterránea en la CMM proviene de dos fuentes principales: 1) infiltración de agua meteórica, y 2) migración ascendente de aguas salinas profundas derivadas de formaciones cretácicas. El agua meteórica se infiltra a lo largo del margen oriental de la cuenca y migra a través de la Formación Mugrosa, donde la interacción agua-roca altera progresivamente su composición química, incrementando notablemente las concentraciones de sodio, calcio y potasio. Las aguas connatas procedentes de formaciones cretácicas subyacentes ascienden a lo largo de planos de fallas inversas, mezclándose con las aguas meteóricas y modificando sus composiciones químicas e isotópicas. Esta mezcla produce un incremento en las concentraciones de cloruro y un enriquecimiento relativo en $\delta^{18}O$ respecto a los valores de la línea meteórica local.

Palabras clave: Isótopos radiogénicos ($^{87}Sr/^{86}Sr$), Isótopos estables ($\delta^{18}O$, $\delta^{2}H$), Mezclas de aguas, Aguas meteóricas, Aguas connatas.

1. Introduction

During the hydrogeological cycle, surface water and groundwater interact and eventually mix depending on several factors such as topography, geology, temperature, altitude, and other environmental conditions. This interaction can lead to either abrupt or gradual changes in the chemical and isotopic composition of the water (*e.g.,* Clark and Fritz, 1997).

Stable isotopes are widely used in hydrogeology and hydrogeochemistry as tools to assess potential changes in chemical composition, determine the origin of water, flow direction patterns, mixing processes, and identify recharge and discharge zones in both surface and groundwater aquifers (*e.g.,* Dansgaard, 1964; Hem, 1989; Fetter, 1994; Hitchon *et al.*, 1999; Fitts, 2002; Dickin, 2018). Radiogenic isotopes, on the other hand, provide valuable insights into relative or absolute residence times and aquifer renewal rates (*e.g.,* Burke *et al.*, 1982; DePaolo and Ingram, 1985; Veizer, 1989; Farrell *et al.*, 1995).

This study focuses on the central region of the Middle Magdalena Basin (MMB) in Colombia, a mature hydrocarbon province with a cumulative oil production of 2.75 billion barrels as of December 2021 (*e.g.,* Pastor-Chacón *et al.*, 2023) and an estimated annual cumulative production of approximately 11.7 million barrels of oil as of December 2024 (Agencia Nacional de Hidrocarburos, 2024). While many oil fields in the MMB historically exhibit low water cuts (typically <10%), current production relies increasingly on enhanced oil recovery (EOR) techniques, such as water injections, to offset reservoir depletion. The basin is also characterized by intense tectonic deformation, with fault systems potentially acting as critical pathways for natural fluid migration (*e.g.,* hydrocarbons, connate waters) and anthropogenic fluid movement (*e.g.,* injected water, flowback from hydraulic fracturing) (Castelblanco *et al.*, 2025). However, the origin of water in production systems, whether naturally infiltrated meteoric water, connate formation water, or EOR-derived fluid, remains poorly understood. This research addresses this gap by investigating groundwater's isotopic and geochemical signatures in the Oligocene Mugrosa Formation, aimed at disentangling their possible

sources and evaluating the role of fault-controlled hydrologic connectivity in fluid redistribution.

Waterflooding has been used as a secondary recovery method in five commercial oil fields within the MMB: La Cira, Galán, Casabe, Yariguí-Cantagallo, and Infantas (Castro *et al.*, 2010). Recently, EOR techniques have been initiated as pilot projects in several of these fields (*e.g.*, Yariguí-Cantagallo, Casabe, Chichimene, and La Cira-Infantas) to improve volumetric sweep efficiency and increase overall recovery factors (Gutiérrez *et al.*, 2024).

Hydrogeological understanding of the MMB has evolved significantly over the past two decades through regional investigations. In fact, several government institutions, including IDEAM (Institute of Hydrology, Meteorology, and Environmental Studies of Colombia) (Vargas *et al.*, 2013; García *et al.*, 2014), the Colombian Geological Service (Hincapié *et al.*, 2004), and the Autonomous Regional Corporation of Central Antioquia (Mejía, 2008), have conducted studies to assess groundwater aquifers in the MMB. A foundational study by Hincapié *et al.,* (2004) classified hydrogeological units based on aquifer productivity, porosity, and permeability, employing the nomenclature established by the International Association of Hydrogeologists (IAH). However, it was not until a decade later that hydrogeological provinces across Colombia were systematically delineated and classified according to tectonostratigraphic frameworks and structural boundaries (Vargas *et al.*, 2013).

Mejía (2008) evaluated groundwater quality and hydrogeochemical facies in the MMB, reporting a predominance of sodium-bicarbonate waters with localized occurrences of calcium-bicarbonate facies. García *et al.*, (2014), expanded on this by characterizing the aquifer systems of the Neogene Real Group and Mesa Group. These units comprise unconfined and semi-confined multilayer aquifers within recent alluvial and fluvial terrace deposits adjacent to the Magdalena River, as well as poorly consolidated detrital sediments. Infiltration rates in these units range from 0 to 500 mm/year, with saturated thicknesses between 80 and 230 m and transmissivity values from 100 to 200 m²/day. More recently, Malagón (2017) and Malagón *et al.* (2021) applied principal component analysis and hierarchical clustering to 140 groundwater samples, offering a refined geochemical classification. Their findings confirmed calcium-bicarbonate waters as the dominant components throughout the basin, with sodium-bicarbonate and chloride types limited to specific areas.

Flow dynamics in shallow aquifers (250-365 m) of the Real Group and Mesa Group were investigated by Piña *et al.* (2022) using stable isotope analyses. Their results revealed seasonal isotopic variability indicative of varying groundwater residence times, surface-groundwater interactions, and regional flow regimes driven by hydraulic gradients. This study also provided evidence of hydraulic connectivity along fractured zones of the Eastern Cordillera, highlighting significant data gaps regarding geology and structures, as well as the lack of long-term groundwater monitoring.

This paper explores the interaction between meteoric and brine waters of the Mugrosa Formation reservoirs through percolation. We hypothesize that meteoric water infiltration primarily occurs through the flanks of the main structures in the area and along fault zones, reaching depths of approximately 1,950 m. These interactions result in an increase of $\delta^{18}O$ and a decrease in the pH of reservoir samples. Other infiltration mechanisms may involve seal leakages and the tortuosity of the overlying formations. The findings obtained in this research are hoped to benefit water management strategies in oil-producing basins.

2. Geological setting

The Middle Magdalena Basin (MMB) is located along the Magdalena River valley, between the Central and Eastern Cordilleras in the Colombian Andes. It is currently classified as an intermontane basin (Sarmiento, 2011) (Fig. 1). The northern boundary is El Banco uplift, the northeastern boundary is the Bucaramanga-Santa Marta Fault, the southeastern boundary is the La Salina and Bituima thrust faults, the southern boundary is the Ibague Fault, and the western boundary is the Mesozoic igneous and metamorphic basement of the Central Cordillera. The study area is located close to the southeastern boundary, where the La Salina thrust fault system has generated several fault propagation folds, notably the Nuevo Mundo Syncline (NMS), the Lisama-Provincia anticlines, and the Peña de Oro syncline. Additionally, folds (both synclines and anticlines) related to the Arrugas and Casabe thrust faults can be found toward the western flank of the basin (Morales *et al*., 1958; Dengo and

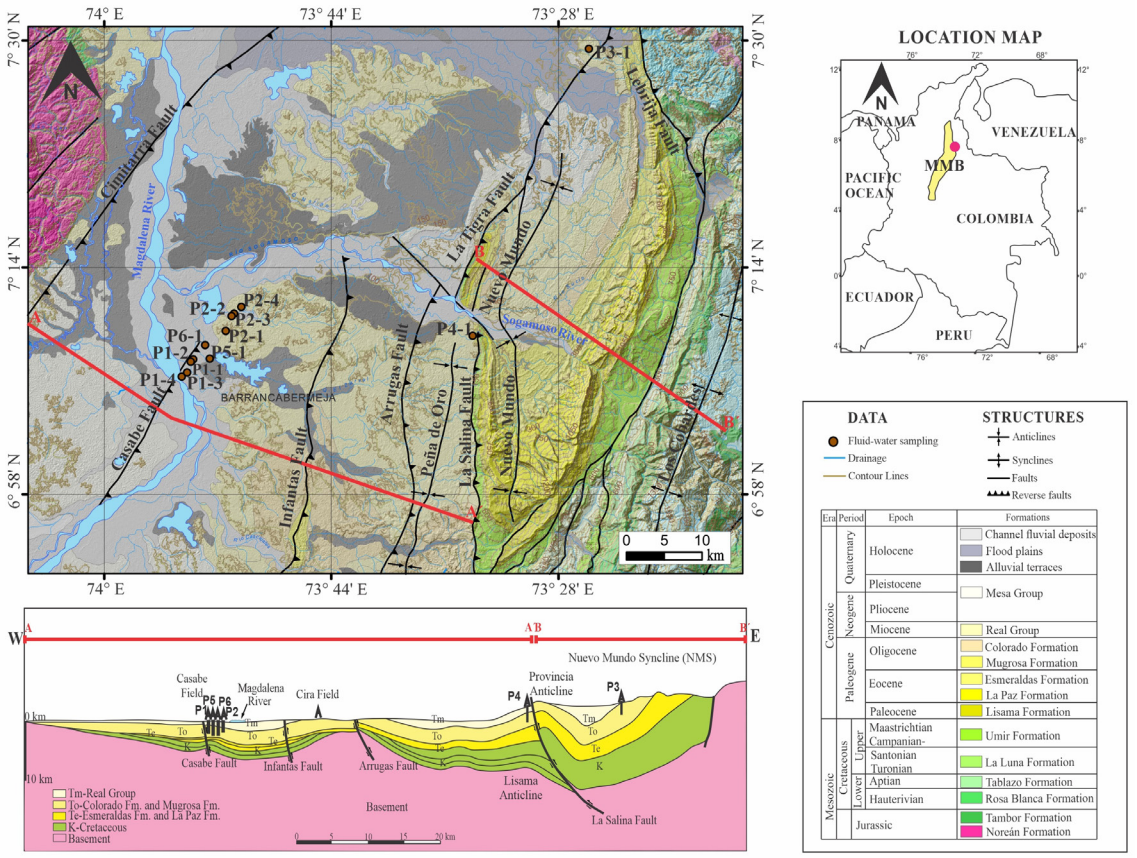

FIG. 1. Location of the study area, sampling sites, and regional schematic cross-section across the sampling areas. The schematic cross-section was adapted from Morales *et al.* (1958) and Gómez *et al.* (2005a, b). **MMB**: Middle Magdalena Basin.

Covey, 1993; Cooper *et al.*, 1995; Gómez *et al.*, 2003, 2005a; Caballero, 2010; Sarmiento, 2011).

Multiple petroleum systems have been identified in the MMB. The Rosa Blanca and Tablazo formations (Lower Cretaceous), and the La Luna Formation (Upper Cretaceous), are recognized as primary source rocks, while the Lisama, La Paz, Esmeraldas, Mugrosa, and Colorado formations (Paleocene to Oligocene) serve as the main reservoir rocks identified to date (Fig. 1). The claystone-rich intervals within the Esmeraldas and Colorado formations act as the primary regional seals for the Cenozoic reservoirs (Morales *et al.*, 1958; Barrero *et al.*, 2007; García *et al.*, 2009; Sarmiento, 2011) (Fig. 1).

The Mugrosa Formation comprises thick, laterally continuous sandstone packages interbedded with shale layers, reflecting high-energy fluvial to deltaic depositional environments. Its total thickness ranges from approximately 500 to 800 m. This formation is unconformably overlain by the Colorado Formation and underlain by the Esmeraldas Formation (Caballero, 2010; Sarmiento, 2011). The Mugrosa and Colorado formations represent alluvial syntectonic deposits, ranging from alluvial fans (on the west) to meandering rivers (on the east), deposited during the Paleogene and Neogene uplift of the basin (Caballero, 2010).

Structural interpretations by Gómez *et al.* (2003, 2005a, 2005b), Caballero (2010), Sarmiento (2011), and Pastor-Chacón *et al.* (2023) suggest that the La Salina and Casabe thrust faults controlled the formation of the Lisama anticline as well as the NMS as fault propagation folds. The La Salina thrust fault system also controlled the formation of fault propagation folds and the syntectonic sedimentation of the Mugrosa and Colorado formations, which were deposited with sediments derived from the Serranía de los Cobardes and the Lisama anticlines at the foothills of the Eastern Cordillera

(Gómez *et al.*, 2003, 2005a, b; Caballero, 2010; Sarmiento, 2011) (Fig. 1). This fault system has been suggested as the main migration pathway of petroleum and connate water from Cretaceous source rocks to the Paleogene reservoir rocks, including the Mugrosa and Colorado formations (Dengo and Covey, 1993; Cooper *et al.*, 1995; Rangel *et al.*, 1996; Ramón *et al.*, 1997, 2001; Gómez *et al.*, 2003, 2005a; Caballero, 2010; Sarmiento, 2011; Pastor-Chacón *et al.*, 2023; Rivera *et al.*, 2025) (Fig. 1).

3. Materials and methods

Formation water samples were collected from twelve producing wells completed in the Mugrosa Formation, at operational depths ranging from 800 to 1,950 m (Fig. 1). These wells are unaffected by EOR operations, ensuring that the geochemical data represented the natural, unaltered conditions of the reservoir. Sampling was conducted in two study areas: 1) the eastern sector-NMS, and 2) the western sector-Casabe field. We collected each sample in pre-cleaned, sterilized amber glass bottles equipped with cap-seals and refrigerated immediately to minimize alterations in chemical composition. Samples containing both hydrocarbon and water phases were separated using a separation funnel.

3.1. Physicochemical analysis

Both in situ and laboratory measurements of physicochemical parameters were conducted. These parameters include total dissolved solids (TDS), conductivity, pH, and temperature. In situ measurements were obtained using a WTW 2E30-101B02 multiparameter instrument, whereas laboratory analyses employed a two-channel HANNA multiparameter instrument for measuring pH, oxidation-reduction potential, and specific ion measurements (pH-ORP-ISE), and total dissolved solids (TDS)-Salinity-resistivity (Tables 1 and 2).

3.2. Chemical analysis

Ion concentration, reported in tables 1 and 2, includes the following major cations: Na^+, K^+, Ca^{2+}, Mg^{2+}, Fe^{2+}, Sr^{2+}, Al^{3+}, and Mn^{2+}, as well as major anions: Cl^-, HCO_3^-, CO_3^{2-}, SO_4^{2-}, and S^{2-}. Cation concentrations were determined using a flame atomic absorption spectrophotometer (Agilent A240S) equipped with an air-acetylene-nitrous oxide flame. Prior to every analysis, the samples underwent standard digestion with concentrated nitric acid, following method SM3030E.

Chloride concentrations were determined by potentiometric titration using silver nitrate ($AgNO_3$) as the titrant. Sulfide concentrations were determined using the iodometric-potentiometric method (SM 4500 S^{2-}-F). A 25 mL sample aliquot was acidified with 2 mL of 6N HCl and subsequently titrated with 0.025N sodium thiosulfate ($Na_2S_2O_3$). Sulfate concentrations were established using the standard turbidimetric method (SM 4500 SO_4^{2-}-E). A 25 mL sample aliquot was mixed with a pH buffer, followed by the addition of 0.1 g of $BaCl_2$. The mixture was stirred and left to rest for 5 minutes before measurement. Carbonate and bicarbonate concentrations were determined by titration. A 25 mL sample aliquot was titrated with 0.02N NaOH until the final endpoint, using phenolphthalein and methyl red as indicators.

Total acids (or total acid number, TAN) were determined by titration with NaOH until neutralization. The NaOH concentration used, along with the formation of salts and the dissociation of organic acids reacting with NaOH, was analyzed to quantify total acidity.

3.3. Stable isotope analysis ($\delta^{18}O$ and $\delta^{2}H$)

Stable isotopes of oxygen ($\delta^{18}O$) and deuterium ($\delta^{2}H$) were analyzed in refrigerated samples at the Beta Analytic-Testing Laboratory in Miami, USA. The analysis was conducted using cavity ring-down spectroscopy (CRDS). A 1.6 mL aliquot of each liquid sample was placed in a vial with a screw cap and septum, then injected into the Picarro L2140-I vaporizer for measurement by CRDS. To ensure high precision, the CRDS system generated six measurement peaks per sample, each lasting nine minutes. Due to potential isotopic memory effects between consecutive samples, only the average of the last three injections was used for final calculations. We used a minimum of three sets of reference standards (*e.g.,* EVIAN, LOUSE, and USGS 50) covering the $\delta^{18}O$ and $\delta^{2}H$ spectrum to bracket the samples. These standards established a linear calibration curve to normalize the $\delta^{18}O$ and $\delta^{2}H$ values on the Vienna Standard Mean Ocean Water (VSMOW) scale. The standard deviation of all analyses was ±0.03. The results are reported in table 3.

TABLE 1. PHYSICOCHEMICAL CHARACTERIZATION (MG/L) OF THE GROUNDWATER ASSOCIATED WITH THE MUGROSA FORMATION (RESERVOIR), MMV BASIN, COLOMBIA.

ID	Depth (m)	Physicochemical characterization				Chemical characterization													
						Cations								Anions					
		pH	Temperature (°C)	Electric conductivity (mS/cm)	Total dissolved solids (TDS) (ppm)	Na^{+} (mg/L)	K^{+} (mg/L)	Mg^{2+} (mg/L)	Ca^{2+} (mg/L)	Sr^{2+} (mg/L)	Fe^{2+} (mg/L)	Mn^{2+} (mg/L)	Al^{3+} (mg/L)	Cl^{-} (mg/L)	HCO_3^{-} (mg/L)	CO_3^{2-} (mg/L)	Sulfates SO_4^{2-} (mg/L)	Sulphides S^{2-} (mg/L)	Organic acids (mg/L)
P1-1	1,828	6.89	26.5	70.6	39,290	20,691	49.67	129.55	4,097.5	278.38	0.88	8.37	0.5	23,216.01	56.95	0	2.17	1	25,198.9
P1-2	1,828	6.54	26.3	72.3	36,730	19,657	54.83	191.43	3,762.5	265	2.4	11.24	0.5	22,693.71	73.22	0	16.28	2.62	23,871.68
P1-3	1,828	6.04	26.4	67.1	34,180	18,261	46.3	134.91	6,235	268.63	11.12	9.27	0.5	23,158.16	40.68	0	37.89	6.1	24,926.05
P1-4	1,828	6.23	26.3	55.1	21,210	12,280	39.83	228.2	3,610	135.38	1.64	7.89	0.5	17,591.27	36.61	0	3.81	1	16,266.83
P2-1	1,798	6.41	26.0	75.3	37,220	16,328	56.74	216.78	5,775	357.25	1.1	12.31	0.5	25,586.43	73.22	0	4.31	1	22,674.46
P2-2	1,798	6.8	25.8	67.5	38,480	15,013	84.46	283.95	3,927.5	338.63	2.17	3.35	0.5	21,809.82	109.83	0	19.89	3.2	19,543.73
P2-3	1,798	6.8	25.8	78.2	31,640	21,019	195.71	332.95	3,172.5	431	0.98	0.71	0.5	26,631.02	113.9	0	81.11	13.06	25,039.45
P2-4	1,798	6.72	25.9	67.5	34,250	13,916	63.39	282.2	2,930	317.13	1.51	2.74	0.5	22,010.71	101.69	0	13.44	2.16	17,411.78
P3-1	793	7.65	25.8	9.01	4,640	4,165	14.22	41.18	107.40	5.01	0.48	0.2	0.5	3,931.21	448.67	45.3	20.23	3.26	3,840.02
P4-1	1,463	8.1	26.0	34.5	9,495	11,111	141.33	122.73	81.75	20.78	0.26	0.2	0.5	12,992	430.68	49.59	43.24	6.96	10,998.28
P5-1	1,951	6.21	26.1	75.0	20,740	20,482	67.26	154.49	5,800	356.63	1.56	15.31	0.5	24,823.07	77.29	0	4.49	1	26,800.46
P6-1	1,951	6.00	25.7	78.4	37,370	20,595	42.6	151.05	4,422.5	272.88	4.45	11.61	0.5	27,233.67	44.75	0	11.91	1.92	25,455.84

TABLE 2. PHYSICOCHEMICAL CHARACTERIZATION (MEQ//L) OF THE GROUNDWATER ASSOCIATED WITH THE MUGROSA FORMATION (RESERVOIR), MMV BASIN, COLOMBIA.

ID	Depth (m)	Physicochemical characterization				Chemical characterization													
						Cations								Anions					
		pH	Temperature (°C)	Electric conductivity (mS/cm)	Total dissolved solids (TDS) (ppm)	Na^{+} (meq/L)	K^{+} (meq/L)	Mg^{2+} (meq/L)	Ca^{2+} (meq/L)	Sr^{2+} (meq/L)	Fe^{2+} (meq/L)	Mn^{2+} (meq/L)	Al^{3+} (meq/L)	Cl^{-} (meq/L)	HCO_3^{-} (meq/L)	$CO3^{2-}$ (meq/L)	Sulfates SO_4^{2-} (meq/L)	Sulphides S^{2-} (meq/L)	Organic acids (meq/L)
P1-1	1,828	6.89	26.5	70.6	39,290	899.61	1.27	10.66	204.88	6.35	0.05	0.3	0.03	654.89	0.93	0	0.05	0.06	467.21
P1-2	1,828	6.54	26.3	72.3	36,730	854.65	1.41	15.76	188.13	6.05	0.13	0.41	0.03	640.16	1.2	0	0.34	0.15	424.66
P1-3	1,828	6.04	26.4	67.1	34,180	793.96	1.19	11.1	311.75	6.13	0.6	0.34	0.03	653.26	0.67	0	0.79	0.36	469.81
P1-4	1,828	6.23	26.3	55.1	21,210	533.91	1.02	18.78	180.5	3.09	0.09	0.29	0.03	496.23	0.6	0	0.08	0.06	240.71
P2-1	1,798	6.41	26.0	75.3	37,220	709.91	1.45	17.84	288.75	8.15	0.06	0.45	0.03	721.76	1.2	0	0.09	0.06	303.52
P2-2	1,798	6.8	25.8	67.5	38,480	652.74	2.17	23.37	196.38	7.73	0.12	0.12	0.03	615.23	1.8	0	0.41	0.19	264.98
P2-3	1,798	6.8	25.8	78.2	31,640	913.87	5.02	27.4	158.63	9.84	0.05	0.03	0.03	751.23	1.87	0	1.69	0.77	359.29
P2-4	1,798	6.72	25.9	67.5	34,250	605.04	1.63	23.23	146.5	7.24	0.08	0.1	0.03	620.89	1.67	0	0.28	0.13	160.85
P3-1	793	7.65	25.8	9.01	4,640	181.09	0.36	3.39	5.37	0.11	0.03	0.01	0.03	110.89	7.36	1.51	0.42	0.19	70.0
P4-1	1,463	8.1	26.0	34.5	9,495	483.09	3.62	10.1	4.09	0.47	0.01	0.01	0.03	366.49	7.06	1.65	0.9	0.41	124.91
P5-1	1,951	6.21	26.1	75.0	20,740	890.52	1.72	12.72	290	8.14	0.08	0.56	0.03	700.23	1.27	0	0.09	0.06	502.1
P6-1	1,951	6.0	25.7	78.4	37,370	895.43	1.09	12.43	221.13	6.23	0.24	0.42	0.03	768.23	0.73	0	0.25	0.11	367.6

TABLE 3. ISOTOPE CHARACTERIZATION ($\delta^{18}O$; $\delta^{2}H$ AND $^{87}Sr/^{86}Sr$) OF THE GROUNDWATER ASSOCIATED WITH THE MUGROSA FORMATION (RESERVOIR), MMV BASIN, COLOMBIA.

ID	Depth (m)	Stable isotope ratio		Sr isotope ratio
		$\delta^{18}O$ (‰)	$\delta^{2}H$ (‰)	$^{87}Sr/^{86}Sr$
P1-1	1,828	-0.28	-21.93	0.708265
P1-2	1,828	-0.37	-21.58	0.708089
P1-3	1,828	-0.6	-22.25	0.708508
P1-4	1,828	-1.87	-25.41	0.709098
P2-1	1,798	-0.29	-21.23	0.708343
P2-2	1,798	-0.74	-24.4	0.708807
P2-3	1,798	0.11	-18.63	0.709675
P2-4	1,798	-0.48	-21.18	0.708624
P3-1	793	-5.14	-26.28	0.708185
P4-1	1,463	-1.54	-17.56	0.712138
P5-1	1,951	-0.17	-21.16	0.708158
P6-1	1,951	0.65	-19.85	0.708033

3.4. Radiogenic isotope analysis ($^{87}Sr/^{86}Sr$)

Radiogenic isotope analysis ($^{87}Sr/^{86}Sr$) was conducted at the Center for Geochronology and Isotope Geochemistry at the Complutense University of Madrid, Spain. The analysis required a specific pretreatment process depending on the Sr ion concentration determined by conventional analysis. For each sample, 10 to 20 mL was evaporated in a clean Teflon crucible on a heating plate at temperatures below 80 °C. The residue was then re-dissolved in 2 mL of HNO_3 Suprapur®, followed by a second evaporation at 120 °C. After drying, 3 mL of 3M HNO_3 was added to facilitate chromatographic separation.

Chromatographic separation of Sr was performed using Sr-Resin™ (Triskem International), which contains crown-ether (4,4'(5')-di-t-butyl cyclohexane-18-crown-6). Sr was then eluted using 0.05M HNO_3, and the Sr-concentrated fraction was identified and evaporated to dryness. The final analysis was conducted using thermal ionization mass spectrometry (TIMS).

The $^{87}Sr/^{86}Sr$ ratios were normalized to a measured value of 0.1194 to correct for potential mass fractionation that may have occurred during filament loading and instrumental analysis. Additionally, the Sr isotope standard NBS 987, which has a certified $^{87}Sr/^{86}Sr$ ratio of 0.710248±0.000003 (per the NBS 1982 Certificate of Analysis, Standard Reference Material 987), was analyzed repeatedly. From nine replicates, a standard deviation (STDEV) of 0.000021 was obtained. The results are reported in table 3.

3.5. Meteoric water line (global and local)

This study used the equation proposed by Harmon Craig in 1961 for the Global Meteoric Water Line (GMWL) (Craig, 1961). The Local Meteoric Water Line (LMWL) was constructed using data collected near the study area, obtained from the International Atomic Energy Agency (IAEA) through its WISER program (Water Isotope System for data analysis, visualization, and Electronic Retrieval) from the 2020-2021 dataset (https://nucleus.iaea.org/wiser).

For the construction of the Local Meteoric Water Line (LMWL), $\delta^{18}O$ and $\delta^{2}H$ data from the past 30 years were analyzed, specifically selecting values from the MMB. This study therefore presents, for the first time, a meteoric water line for the central region of the MMB (*e.g.,* the La Fortuna and Lisama areas), providing a valuable framework for interpreting the isotopic fractionation processes affecting meteoric water and groundwater in the basin.

4. Results

4.1. Physicochemical analysis of groundwater

The samples analyzed exhibit different physicochemical parameters depending on their sampling location within the basin (Fig. 2; Tables 1 and 2):

Eastern area-NMS: The groundwater samples here show a higher pH, ranging from 7.65 to 8.10. Electrical conductivity values are lower than in the western area, with 9.01 mS/cm for sample P3-1 and 34.50 mS/cm for sample P4-1. Similarly, TDS values are also lower, ranging between 4,640 ppm (P3-1) and 9,495 ppm (P4-1). Temperature differences are minimal, ranging between 25.8 °C and 26.0 °C.

Western area-Casabe field: Groundwater in this region has a pH ranging from 6.00 to 6.89, an electrical conductivity between 55.10 and 78.40 mS/cm, TDS values between 20,740 ppm and 39,290 ppm, and temperatures between 25.7 °C and 26.5 °C.

4.2. Chemical analysis

Piper diagrams serve as a graphical tool for classifying groundwater based on its chemical composition by organizing ion concentrations (cations and anions) (Piper, 1944). This analysis allows for the identification of two key aspects: 1) The origin of dissolved ions in the water; and 2) The evolution of the water's chemical composition due to water-rock interactions in the Mugrosa Formation.

According to the Piper classification diagram, the groundwater in the study area is predominantly of the sodium-chloride type (Fig. 3). Two distinct subgroups are identified, corresponding to samples from the Eastern area-NMS and the Western area-Casabe field. Within each subgroup, samples can be further distinguished according to their ionic concentrations, indicating consistent geochemical signatures for each area. The Eastern area-NMS samples are relatively enriched in HCO_3 and CO_3 relative to Ca and Mg, whereas the Western area-Casabe samples show the opposite trend, with a marked increase in Cl concentrations toward the west (Fig. 3).

Gibbs diagrams illustrate the relationship between TDS concentration and the proportions of cations (Na/(Na+Ca)) and anions ($Cl/(Cl+HCO_3)$) in groundwater (Gibbs, 1970). These diagrams help identify the dominant processes influencing the chemical composition of groundwater, which include: 1) Meteoric water (influence of rainwater infiltration); 2) Water-rock interaction (*e.g.,* dissolution, ion exchange, and mineral alteration); and 3) Mineral precipitation (increased salinity due to temperature-driven evaporation) (Fig. 4).

The physicochemical characteristics of groundwater enable us to predict its evolution and flow within the system (Chebotarev, 1955; Mifflin, 1988; Bustamante, 2017); however, the groundwater flow trajectories are primarily dominated by the hydrostatic gradient and geological factors (*e.g.,* faulting, structures) of the studied area. Several studies (Mifflin, 1988; Clark and Fritz, 1997; Cook and Herczeg, 2000; Bustamante, 2017; Malagón *et al.*, 2021; Piña *et al.*, 2022) have shown that the calcium-bicarbonate-type waters transition to sulfate and chloride waters as depth increases in the infiltration process in the subsurface (Fig. 5).

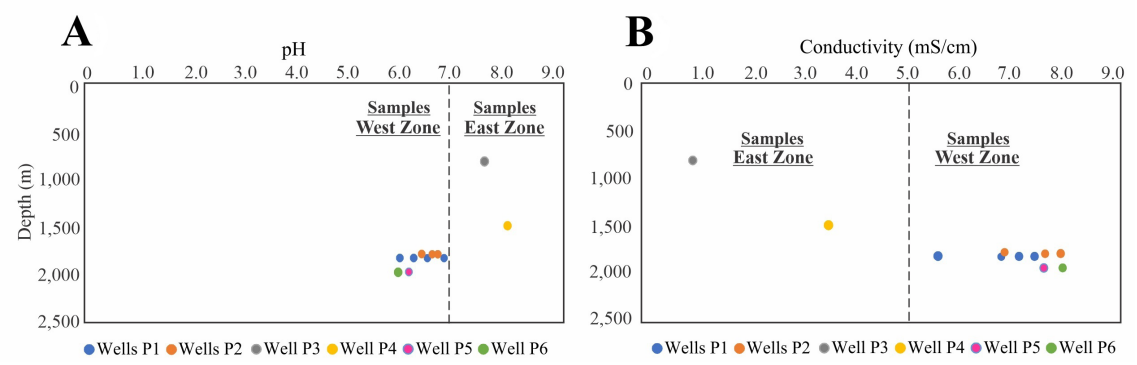

FIG. 2. Physicochemical characteristics of groundwater in the MMB area. **A.** Depth versus pH. **B.** Depth versus electrical conductivity. The samples have been grouped based on whether they belong to the western or eastern sectors of the study area.

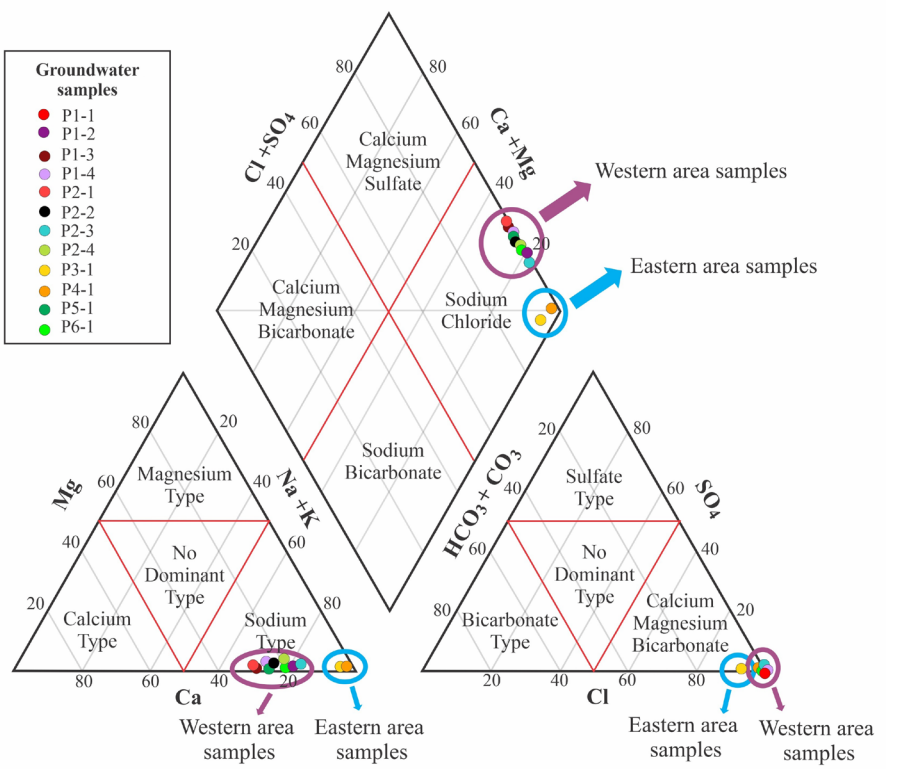

FIG. 3. Piper diagram showing the spatial distribution of groundwater types in the Mugrosa Formation. Eastern area-NMS samples (P3-1 and P4-1) have relatively higher concentrations of bicarbonate (HCO_3) and carbonate (CO_3) compared to calcium (Ca) and magnesium (Mg), whereas Western area-Casabe field samples show higher chloride (Cl) concentrations. The diagram highlights the contrasting geochemical signatures and spatial zonation of groundwater across the study area.

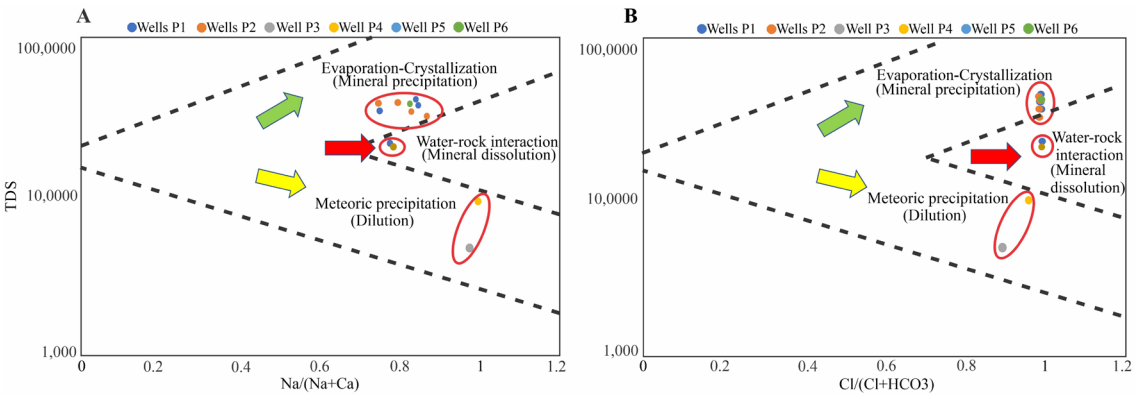

FIG. 4. Gibbs diagrams illustrating geochemical processes controlling groundwater composition in the Mugrosa Formation. **A.** TDS versus (Na/(Na+Ca)); this diagram helps identify whether groundwater chemistry is dominated by atmospheric precipitation, water-rock interaction, or mineral precipitation. **B.** TDS versus Cl/(Cl+HCO_3); this diagram highlights the influence of ion exchange mechanisms or mineral precipitation. Both diagrams suggest that meteoric water infiltration plays a significant role in the water-rock interaction, as observed in the groundwater chemistry of the analyzed samples, particularly in the eastern part of the basin, where lower TDS values and distinct ionic compositions indicate a stronger influence of meteoric water recharge.

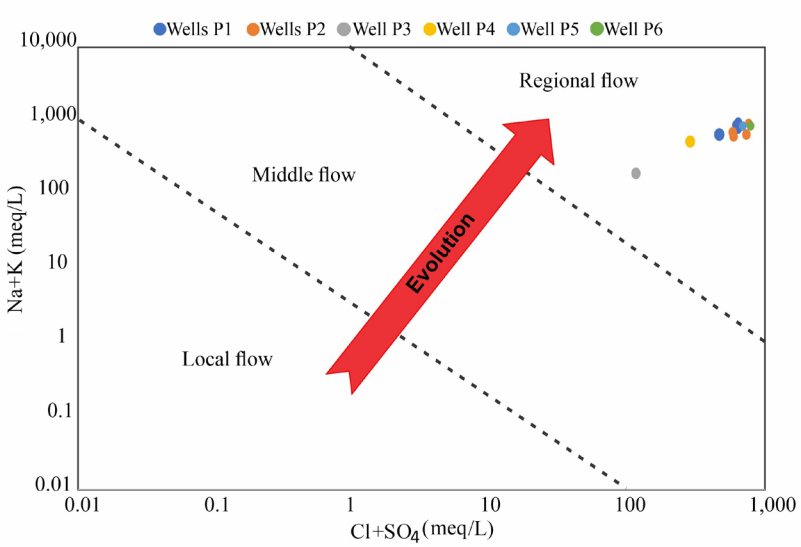

FIG. 5. Mifflin diagram showing the classification of groundwater flow systems (local, intermediate, and regional) based on hydrochemical composition. Groundwater samples from the Mugrosa Formation are plotted to evaluate their possible association with regional flow.

Based on the ionic content present in these waters, previous authors classified the basinal flow patterns as local, intermediate, and regional.

Figure 5 shows that the water samples have compositions possibly related to deep regional flow due to the interaction between groundwater and the reservoir rock (*i.e.*, Mugrosa Formation), as indicated by the analytical results obtained in this investigation.

4.3. Isotope analysis ($\delta^{18}O$, $\delta^{2}H$, $^{87}Sr/^{86}Sr$)

Isotopes are widely used in hydrogeochemical studies, offering insights into physicochemical processes such as evaporation, condensation, and water-rock interactions. Additionally, stable isotopes can contribute to the definition of groundwater flow patterns when combined with conventional ion analyses, while radiogenic isotopes can provide clues about the relative age of basinal waters (Dansgaard, 1964; Hem, 1989; Fetter, 1994; Hitchon *et al.*, 1999; Fitts, 2002; Davis and Elderfield, 2004; Dickin, 2018).

The physicochemical processes affecting groundwater can be analyzed using the δ ($^{2}H/^{1}H$) and δ ($^{18}O/^{16}O$) ratios, which describe variations in the relative abundance of heavier versus lighter stable isotopes. These values are expressed in per mil (‰) relative to Standard Mean Ocean Water (SMOW) (Dansgaard, 1964; Hem, 1989; Fetter, 1994; Hitchon *et al.*, 1999; Fitts, 2002; Dickin, 2018). These isotope ratios help determine whether a sample exhibits isotopic depletion or enrichment in $\delta^{18}O$ and $\delta^{2}H$.

The results, shown in figure 6 and table 3, indicate for the samples from the east area, $\delta^{18}O$ values between -5.14 ‰ and -1.54 ‰ and $\delta^{2}H$ values ranging from -26.28 ‰ to -17.56 ‰. In contrast, the samples from the west area exhibit $\delta^{18}O$ values ranging from -1.87 ‰ to 0.65 ‰ and $\delta^{2}H$ values between -25.41 ‰ and -18.63 ‰.

The $^{87}Sr/^{86}Sr$ ratio can be compared with the $^{87}Sr/^{86}Sr$ composition of seawater over geological time (Burke *et al.*, 1982; DePaolo and Ingram, 1985; Veizer, 1989; Farrell *et al.*, 1995). In the present study, the $^{87}Sr/^{86}Sr$ ratios vary between 0.7081 and 0.7121 in the east area (well depths between 793 and 1,463 m), and between 0.7080 and 0.7097 in the west area (well depths between 1,798 and 1,951 m) (Table 3). These values, together with the stable isotope data illustrated in figure 6, indicate that the western samples are relatively enriched in $\delta^{18}O$ compared to those from the east, suggesting longer residence times and enhanced water-rock interaction in the deeper reservoir intervals. The positive relationship observed between $\delta^{18}O$ and chloride (Cl^{-}), a chemically conservative tracer, further supports mixing between meteoric waters and connate fluids, consistent with regional flow pathways in the Mugrosa Formation.

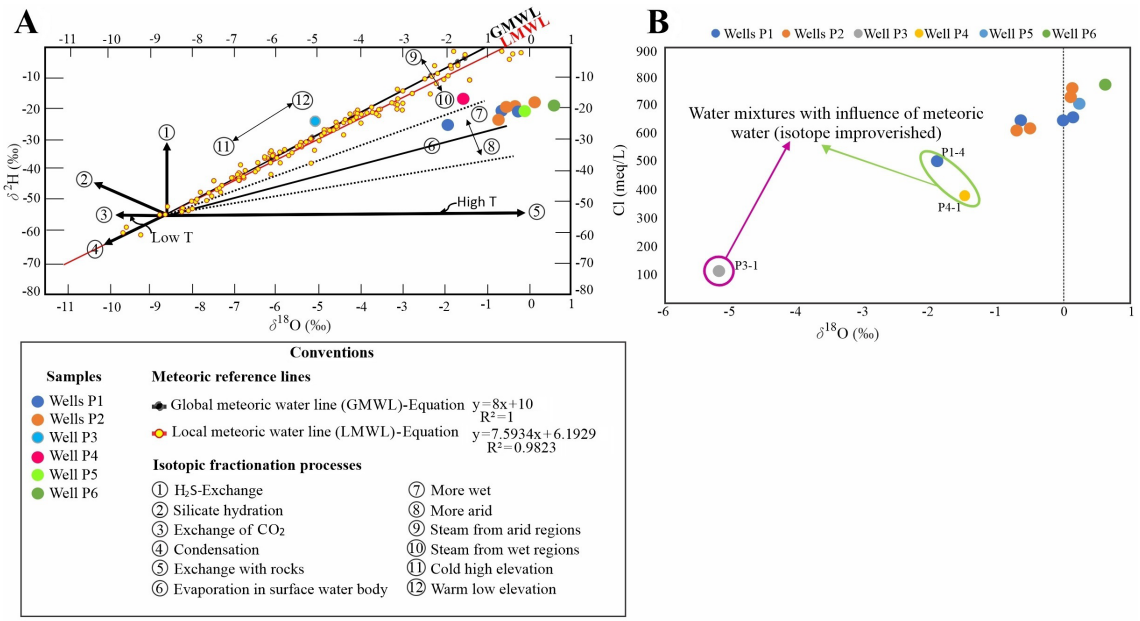

FIG. 6. Stable isotope behavior and isotopic fractionation processes in groundwater from the MMB area. **A.** Variation in δ^2H versus $\delta^{18}O$ values in water samples, showing greater $\delta^{18}O$ enrichment in the western samples compared to those from the eastern area. Tendency lines from Clark and Fritz (1997). **B.** Relationship between chloride (Cl^-) and $\delta^{18}O$. This relationship proved useful for evaluating isotopic fractionation, water-rock interaction processes, and relative groundwater residence time, allowing the distinction between meteoric waters and mixtures of meteoric and connate waters. GMWL and LMWL lines constructed as shown in section 3.5.

5. Discussion

5.1. Hydrogeochemical characteristics of groundwater

5.1.1. Ionic and isotopic correlations

The increasing trend of electrical conductivity with depth (Fig. 2) aligns with the expected geochemical evolution of groundwater in sedimentary basins, where prolonged water-rock interactions at depth enrich the water in dissolved ions, producing brackish compositions. However, the anomalously relatively low pH values in deeper zones challenge conventional models that predict higher pH due to carbonate buffering (Drever, 1982). This discrepancy can be resolved by incorporating the organic acids identified in our analyses (Tables 1 and 2), which are linked to redox reactions during water-hydrocarbon-rock interactions (Surdam *et al.*, 1993; Lundegard and Kharaka, 1994; Palmera, 2023). These acids lower the pH and drive the dissolution of carbonate and feldspar minerals, further modifying ionic balances and enhancing conductivity in a feedback mechanism.

The spatial distribution of water types in the Mugrosa Formation (sodium-chloride type groundwater, with higher Cl^- concentrations in the west and relatively higher HCO_3^- and CO_3^{2-} concentrations in the east) reflects contrasting fluid origins and migration pathways (Fig. 3). In fact, elevated Cl^- concentrations in the western part of the study area correlate with prolonged residence times and mixing with Cretaceous connate waters that ascend via faults, such as La Salina and Casabe (Fig. 1). In contrast, the eastern area's higher pH (7.65-8.10) and carbonate (CO_3^{2-}) and bicarbonate (HCO_3^-) content indicate dominant meteoric recharge near the NMS (Fig. 3). The cation evolution pattern, observed by analyzing the Na/(Na+Ca) and Cl/(Cl+HCO_3) ratios, further supports this model: meteoric waters in the east evolve from sodium-rich compositions to sulfate-dominated and eventually chloride-rich fluids in the west, consistent with progressive water-rock interaction, mineral precipitation, and connate mixing (Chebotarev, 1955; Mifflin, 1988; Clark and Fritz, 1997; Cook and Herczeg, 2000; Schiavo *et al.*, 2009) (Fig. 4).

Cationic ratios provide further evidence of hydrochemical zonation. For example, Na and K dominate over Ca and Mg, with Ca+Mg ratios increasing westward (Fig. 7A), while Na appears to prevail over K during ion-exchange processes associated with water-rock interactions (Fig. 7B). This trend suggests shorter residence times for the eastern samples, as indicated by their lower Cl^- concentrations and lower Cl-(Na+K)/Cl ratios, compared to the western samples (Fig. 7C). The latter may reflect a longer interaction with Cretaceous-derived brines and enhanced mineral dissolution (*e.g.,* carbonates and feldspars) (Hem, 1989; Drever, 1997; Tostado, 2010). Such patterns may reflect the Mugrosa Formation's fluvial architecture (Caballero, 2010; Sarmiento, 2011), that is, coarse-grained channel sands in the east facilitate rapid meteoric infiltration, while finer-grained floodplain deposits in the west prolong fluid-rock contact, enhancing ion exchange and organic acid generation.

5.1.2. Water-rock interaction and relative residence time in the hydrogeological system

The isotopic and geochemical data reveal that the hydrogeological system in the study area is affected by two processes: meteoric water percolation and connate water migration. These processes occur in two different structures (compartments) that are isolated by the Umir Formation, which is the regional seal, and connected through the thrust fault systems (*e.g.,* La Salina, Arrugas, Infantas, Casabe) (Figs. 6 and 8). The interaction between meteoric and connate waters resulting in depleted $\delta^{18}O$ values (-5.14 ‰ in P3-1) and high CO_3^{2-}/HCO_3^- ratios in the eastern area confirms significant meteoric recharge along the eastern flank of the NMS, where short residence times maintain a near-neutral pH (7.65-8.10). Furthermore, the ionic and isotopic composition of groundwater in the eastern area aligns closely with the local and global meteoric water lines established in

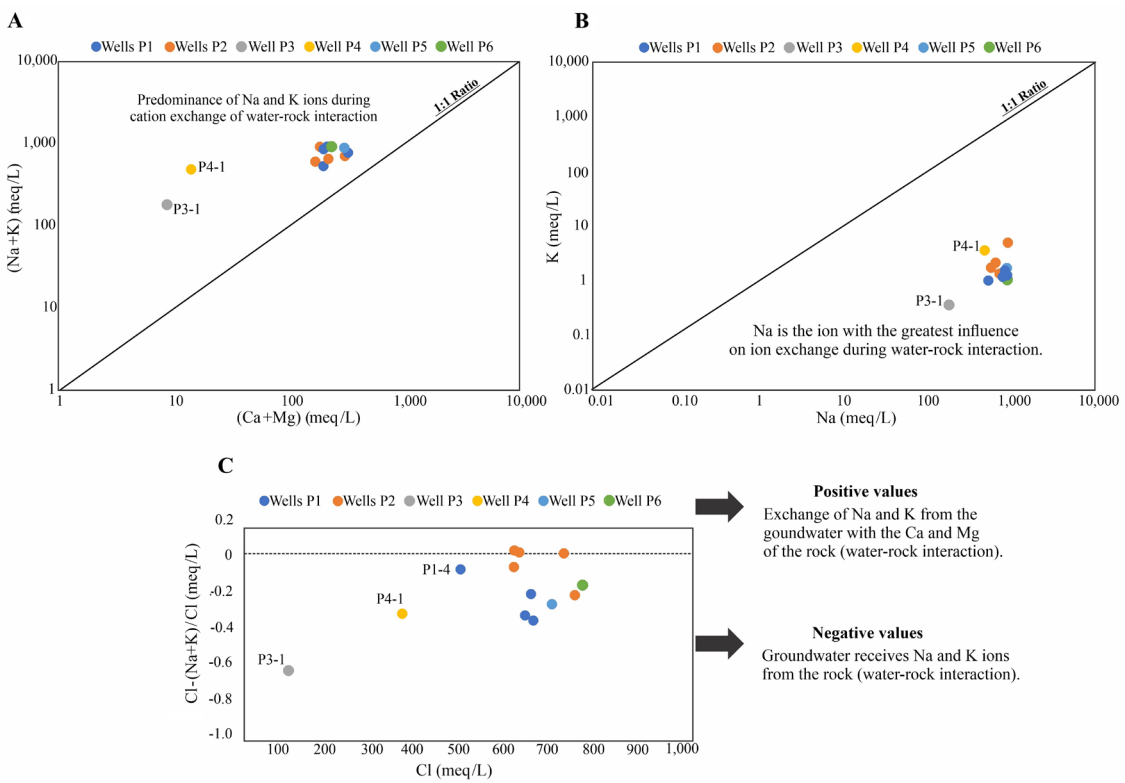

FIG. 7. Ionic relationships indicating dominance patterns and ion exchange processes in groundwater from the Mugrosa Formation: **A.** (Na+K) versus (Ca+Mg) plot, highlighting the dominance of Na and K ions over Ca and Mg. **B.** K versus Na concentrations, illustrating the role of water–rock interactions, with Na typically present in higher concentrations than K. **C.** Exchange bases index plot suggesting an enrichment in Na and K resulting from mineral dissolution and cation exchange with clay minerals.

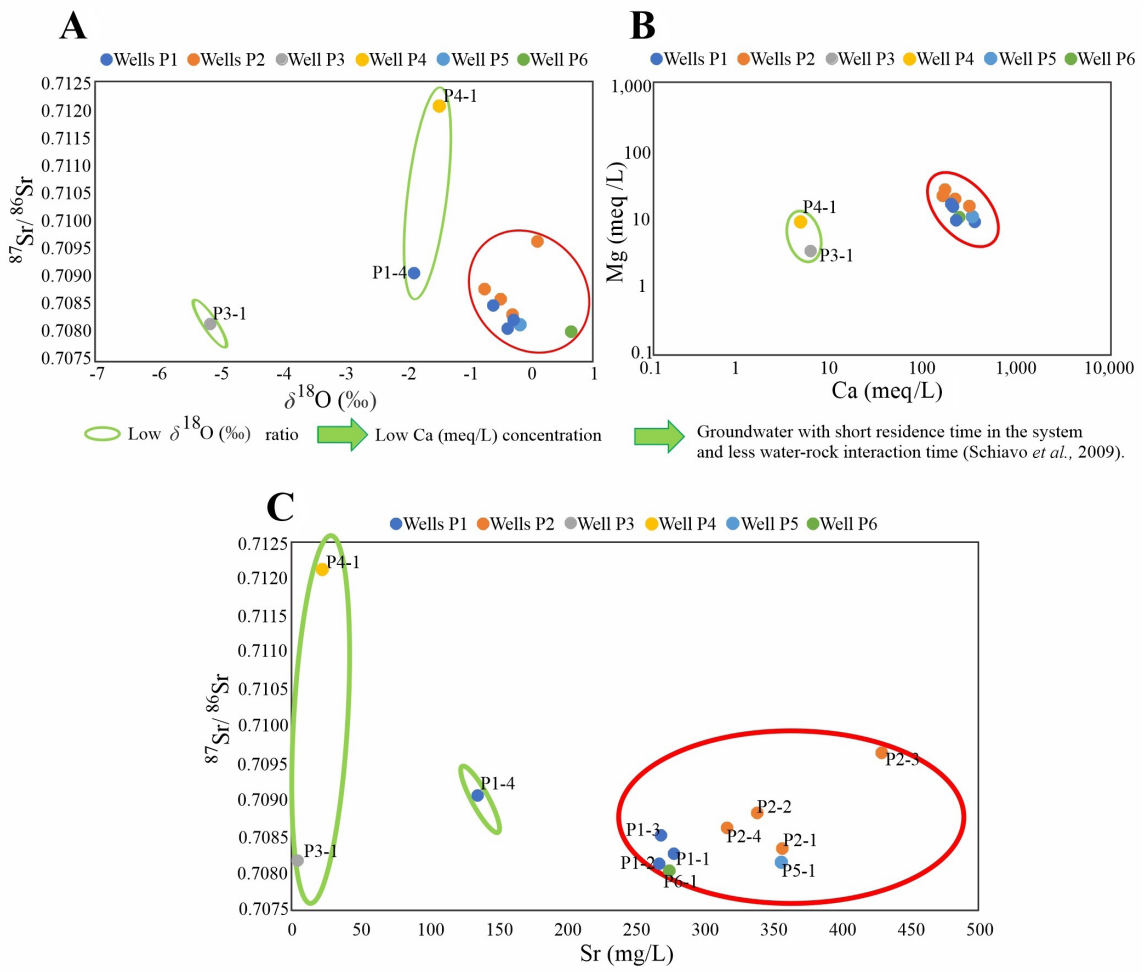

FIG. 8. Ionic and isotopic correlations used to infer groundwater mixing processes and relative residence times. **A.** $^{87}Sr/^{86}Sr$ versus $\delta^{18}O$ plot. Three distinct water groups are identified based on $\delta^{18}O$ values and their spatial association. Group 1 corresponds to meteoric waters from the eastern area, characterized by depleted $\delta^{18}O$ values (sample P3-1), indicative of recent recharge. Group 2 comprises mixed meteoric and connate waters, with intermediate $\delta^{18}O$ values (samples P1-4 and P4-1). Group 3 consists of connate waters from the western area, exhibiting enriched $\delta^{18}O$ values, suggesting prolonged residence times and significant interaction with the host rock. **B.** Mg versus Ca plot for groundwater residence time differentiation. Two distinct groups are recognized: one characterized by elevated Ca concentrations, associated with samples from the western area (wells P1, P2, P5, and P6), and another with lower Ca concentrations, corresponding to the eastern area (wells P3 and P4). Magnesium concentrations remain relatively stable along the y-axis. **C.** $^{87}Sr/^{86}Sr$ versus Sr plot. The observed trend mimics that of panel 8A, delineating three distinct groups. However, in this case, Sr concentrations provide further resolution: eastern samples exhibit lower Sr contents compared to western samples.

this investigation, indicating a predominance of meteoric recharge (Fig. 6A).

The anomalous $^{87}Sr/^{86}Sr$ ratios (*e.g.,* 0.71213 in sample P4-1; Fig. 8A,C), may indicate two key processes (Mearns and McBride, 1999): 1) mixing with Cretaceous connate fluids, where overpressured brines possibly migrate through reverse faults (*i.e.*, La Salina, Arrugas, Casabe) from the La Luna Formation, introducing radiogenic ^{87}Sr (from K-feldspars/micas) and Cl^- (Fig. 6B); and 2) extended water-rock interaction, where organic acid dissolve felspars and carbonates increasing the Na^+/Cl^- and lowering the pH (6.00-6.89), which is consistent with prolonged fluid retention in low-permeability

sediments. However, sample P1-4 from the western area stands out as an exception, exhibiting isotopic characteristics comparable to those of sample P4-1 from the eastern sector, which suggests a pronounced meteoric water influence (Figs. 6 and 8).

The east-west hydrochemical zonation in the MMB is supported by ionic and isotopic trends, including higher exchange-base index values with Cl^-, increasing (Na+K) relative to (Ca+Mg), and a westward increase in Cl^- accompanied by $\delta^{18}O$ enrichment (Figs. 6B, 7A, and 7C). These patterns indicate deeper saline inputs and enhanced silicate alteration, consistent with fluvial depositional controls. In the eastern sector, coarse channel sands facilitate rapid meteoric infiltration, whereas in the west, fine-grained overbank deposits extend residence times and promote ion-exchange processes (Fig. 8A, C). This study demonstrates that the covariations between $^{87}Sr/^{86}Sr$ and $\delta^{18}O$, between $^{87}Sr/^{86}Sr$ and Sr, and between Cl and $\delta^{18}O$ serve as effective geochemical tracers for constraining groundwater origins and residence times.

In the MMB, fault-induced hydrocarbon migration from the La Luna Formation to the Mugrosa reservoirs (Ramón *et al.*, 1997, 2001; Rangel *et al.*, 2000; Thompson-Butler *et al.*, 2019; Pacheco-Mendoza *et al.*, 2024) underpins $\delta^{18}O$-Cl^- covariation, as oil-water-gas multiphase migration (Tissot and Welte, 1984) transports connate fluids, which mix with meteoric waters to reshape regional chemistry. Sample P4-1 shows an anomalous $^{87}Sr/^{86}Sr$ ratio likely due to an enrichment in radiogenic ^{87}Sr. Mearns and McBride (1999) reported that $^{87}Sr/^{86}Sr$ ratios depend on the composition of dissolved minerals; higher ratios are associated with K-feldspars and micas, while lower values correspond to marine carbonate rocks. The anomalous high ratio in sample P4-1 suggests a mixture of meteoric water with oil-related water, which typically has elevated $^{87}Sr/^{86}Sr$ ratios (Veizer, 1989; Mearns and McBride, 1999).

5.2. Groundwater flow paths/regional flow and hydrogeological model

Figure 9 illustrates the proposed flow paths of meteoric water within the Mugrosa Formation in the central MMB. The primary recharge areas are located on the eastern flank of the NMS at elevations between 150 and 200 m above sea level (m a.s.l.), where meteoric water infiltrates westward through the formation. Although the Cenozoic strata dip toward the east, the regional hydraulic gradient, driven by the topographic relief from the Eastern Cordillera foothills (ranging from

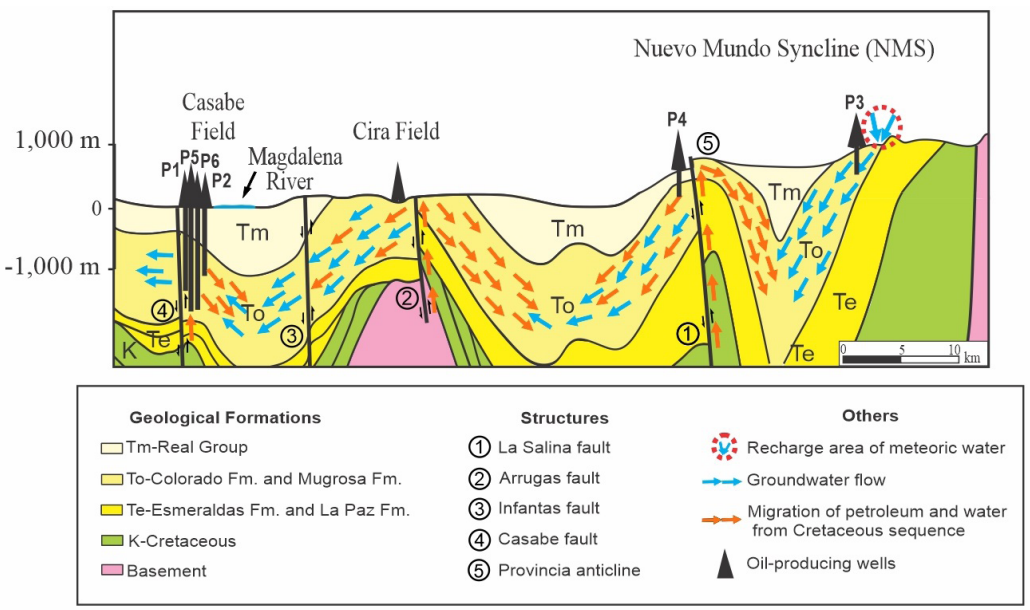

FIG. 9. Conceptual schematic hydrodynamic diagram illustrating recharge areas and potential groundwater flow paths from high to low elevations, together with the upward migration of deep Cretaceous connate waters along reverse fault planes. Diagram adapted and modified from Morales *et al.* (1958) and Gómez *et al.* (2005a, b).

700 to 1,700 m a.s.l.) to the Magdalena River (at an elevation of between 70 and 75 m a.s.l.), governs the direction of groundwater flow. This flow could be further enhanced by permeable fault zones, such as the Arrugas Fault, along with geological outcrops that may serve as secondary infiltration points. Piña *et al.* (2022) described similar processes, albeit in shallower geological formations (depths ranging from 250 to 395 m), such as the Real Group and the Mesa Group (Miocene-Pleistocene), where meteoric water infiltrates through major geological structures. These authors also noted that limited knowledge of these structures and a lack of monitoring hindered the ability to track the infiltration process in the deeper and older formations in the MMB properly.

As the meteoric water moves westward, it descends from the western flank of the NMS and from the Peña de Oro syncline (140 to 150 m a.s.l.) to lower elevations (about 80 m a.s.l.). In this down-path groundwater flow, there is an interaction with connate waters derived from Cretaceous strata that migrate upward along reverse faults, such as the La Salina, Arrugas, Infantas, and Casabe faults. The Umir Formation, which is the regional seal between the Cretaceous and Cenozoic units, isolates the overpressured connate fluids while permitting limited vertical migration through reactivated faults (Rivera *et al.*, 2025). Hydrocarbons and connate waters migrate together as multiphase fluids, but different physical processes govern their movement. Hydrocarbons, being less dense and more buoyant, tend to migrate preferentially along structural pathways, while hydraulic gradients and overpressure primarily drive the movement of brine. This process creates localized mixing zones that can be detected through isotopic anomalies, such as enriched $^{87}Sr/^{86}Sr$ ratios. This interplay between structural architecture, stratigraphic compartmentalization, and hydraulic gradients defines the complex dynamics of groundwater within the MMB.

Geochemical studies by Rangel *et al.,* (1996, 2000), Ramón *et al.,* (1997, 2001), Sarmiento (2011), and Thompson-Butler *et al.,* (2019) confirm that the hydrocarbons found in the MMB originated from Cretaceous source rocks, mainly the La Luna Formation, as indicated by biomarker analyses of saturated and aromatic fractions. These findings support the hypothesis that connate waters migrate alongside hydrocarbons from the La Luna Formation into Cenozoic reservoirs.

Once the connate waters are emplaced, they mix with meteoric water, modifying the hydrogeochemical system. Whilst this mixing process is facilitated by fault-controlled connectivity, it occurs differently over time and through various mechanisms when compared to hydrocarbon migration (Bjørlykke, 1988; Mearns and McBride, 1999). In this case, water movement is less influenced by buoyancy and is primarily driven by pressure differentials and rock-fluid interactions.

Depending on the fault system, the polyphase history of some (*e.g.,* La Salina) may restrict their actual hydraulic connectivity to the Mugrosa Formation reservoirs or deeper strata, despite evidence hinting at it as a pathway for fluid migration (*e.g.,* Castelblanco *et al.*, 2025). As previously mentioned, overpressures in deeper Cretaceous compartments restrict the vertical percolation of meteoric waters; however, seismic pumping may facilitate this process (Simpson, 2024). For example, pressure/permeability tests or other production data from adjacent fault systems could provide additional evidence to support or refute the model proposed in this study.

The hydrogeochemical results obtained here align with the hydrogeological model proposed by Cañas *et al.* (2019) and Piña *et al.* (2022), which also identified a primary infiltration area located in the eastern MMB, with groundwater flow directed westward. While Cañas *et al.* (2019) proposed this flow path for Neogene formations, our study extends this flow pattern to the Paleogene Mugrosa Formation (Fig. 9). The infiltration area for this formation is located in the eastern region at higher elevations, while the discharge area is situated near the Magdalena River. Piña *et al.* (2022) highlighted the lack of structural knowledge and groundwater monitoring in the MMB, and suggested that shallow aquifers associated with Neogene formations exhibited connections between surface and groundwater due to the hydraulic gradient and potential fractures. Our findings provide evidence that meteoric water infiltration occurs at significant depths (between 793 and 1951 m) in the MMB. Additionally, ionic, stable isotope, and radiogenic analyses confirm that groundwater chemistry evolves due to water-rock interactions as it moves through the hydrogeological system. These results also suggest possible connections between regional groundwater flows and deep connate waters from

Cretaceous formations, migrating toward the surface through fault systems, a hypothesis that warrants further investigation.

While the regional groundwater flow pattern (east-to-west) dominates the Mugrosa Formation's hydrodynamics, localized brine systems may arise from structural and stratigraphic heterogeneities. These compartmentalized subsystems, potentially driven by overpressure differentials across the Umir Formation seal, could explain geochemical anomalies (*e.g.*, elevated $^{87}Sr/^{86}Sr$, Cl^- spikes) that deviate from regional trends.

Ultimately, the low water cut levels in production wells throughout the study area indicate complex fluid dynamics, as seals facilitate the selective movement of hydrocarbons while limiting the migration of large volumes of water. Alternative mechanisms for water infiltration and migration from deeper Cretaceous formations into Paleogene reservoirs include the tortuosity of the succession and seal leaks of the regional Umir Formation. All these aspects should be investigated in future research.

6. Conclusions

A key emerging challenge in mature hydrocarbon-producing basins in Colombia, exemplified by the Middle Magdalena Valley Basin (MMB), is the practical application of analytical techniques capable of distinguishing between naturally infiltrated meteoric water, connate formation water, and fluids introduced through enhanced oil recovery (EOR) operations. As EOR processes become increasingly prevalent, they introduce additional geochemical and isotopic complexities to the signatures of groundwater and formation fluids, complicating the interpretation of basinal fluid origins. This problem requires the development of robust methodologies to characterize and trace fluid sources within the reservoir system accurately

This study therefore provides new insights into the hydrogeological and geochemical processes governing groundwater flow in the Mugrosa Formation of the MMB. Geochemical and isotopic data indicate a regional groundwater flow system with recharge occurring at the foothills of the Eastern Cordillera and discharge near the Magdalena River. Groundwater in the eastern MMB shows a stronger meteoric influence, as indicated by higher carbonate and bicarbonate concentrations and less evolved chemical signatures. In contrast, western areas exhibit more evolved waters with elevated chloride (Cl^-) concentrations, as well as enriched $\delta^{18}O$ and $^{87}Sr/^{86}Sr$ isotopic ratios, suggesting longer residence times and greater rock-water interaction. Mixing between meteoric and connate waters occurs mainly along structural features such as thrust faults and folds. Connate waters, derived from deeper Cretaceous units, migrate upward along fault planes with hydrocarbons and interact with meteoric water in Paleogene reservoirs, altering their geochemical and isotopic profiles.

Acknowledgements

The authors acknowledge the Ministry of Science, Technology, and Innovation of Colombia (Minciencias) for its financial support through Grant No. 757 of the 2016 National Doctoral Program. Gratitude is also extended to the Petroleum Geochemistry Laboratory at the Industrial University of Santander and the Thermochronology Research Laboratory at EAFIT University for their valuable analytical support. Special thanks are due to Engineer Jorge Sáchica (ECOPETROL) for his collaborative contributions. The authors further express their sincere appreciation to the anonymous reviewers whose insightful comments and constructive suggestions greatly improved the clarity and overall quality of this paper.

References

Agencia Nacional de Hidrocarburos. 2024. Producción fiscalizada de petróleo por campo (Barriles Por Día Calendario, PDC).

Barrero, D.; Pardo, A.; Vargas, C.; Martínez, J. 2007. Colombian sedimentary basins: Nomenclature, boundaries and petroleum geology, a new proposal. Agencia Nacional de Hidrocarburos: 92 p. Bogotá.

Bjørlykke, K. 1988. Sandstone diagenesis in relation to preservation, destruction and creation of porosity. Developments in Sedimentology 41: 555-588. https://doi.org/10.1016/S0070-4571(08)70180-8

Burke, W.H.; Denison, R.E.; Hetherington, E.A.; Koepnick, R.B.; Nelson, H.F.; Otto, J.B. 1982. Variation of seawater $^{87}Sr/^{86}Sr$ throughout Phanerozoic time. Geology 10 (10): 516-519. https://doi.org/10.1130/0091-7613(1982)10%3C516:VOSSTP%3E2.0.CO;2

Bustamante, E. 2017. Identificación de procesos hidrogeoquímicos aplicando modelación inversa en el acuífero Soconusco, Chiapas. M.Sc. Thesis. Instituto Potosino de Investigación Científica y Tecnólogica: 111 p. San Luis Potosí.

Caballero, V. 2010. Evolución tectono-sedimentaria del Sinclinal de Nuevo Mundo, Cuenca sedimentraia Valle Medio del Magdalena Colombia, durante el Oligoceno-Mioceno. M.Sc. Thesis. Universidad Industrial de Santander: 162 p. Bucaramanga.

Cañas, H.; Pérez, O.; Herrera, W.; Morales, C.; Alvarado, S.; Pineda, C.; Mayorga, L. 2019. Modelo hidrogeológico conceptual del Valle Medio del Magdalena, Planchas 108 y 119, Puerto Wilches, Barrancabermeja, Sabana de Torres y San Vicente de Chucurí. Bogotá. Servicio Geológico Colombiano: https://srvags.sgc.gov.co/PortalWeb/ModeloHidrogeologicoVMM/Documento/PDF/InfoMHCVMMPl108-119.pdf

Castelblanco, C.A.; Vargas, C.A.; Cardozo, N. 2025. Seismic attenuation in the Middle Magdalena Valley, Colombia, and possible relation to fluid lubricated fault zones. Journal of South American Earth Sciences 153: 105359. https://doi.org/10.1016/j.jsames.2025.105359

Castro, R.; Maya, G.; Mercado, D.; Trujillo, M.; Soto, C.; Pérez, H.; Lobo, A.; Ordoñez, A.; Sandoval, J.E. 2010. Enhanced oil recovery (EOR) status-Colombia. *In* SPE Latin American and Caribbean Petroleum Engineering Conference. Lima. https://doi.org/10.2118/139199-MS

Chebotarev, I.I. 1955. Metamorphism of natural waters in the crust of weathering-1. Geochimica et Cosmochimica Acta 8 (1-2): 22-48. https://doi.org/10.1016/0016-7037(55)90015-6

Clark, I.; Fritz, P. 1997. Environmental isotopes in hydrogeology, 1st edition. Lewis Publishers: 328 p. New York.

Cook, P.G.; Herczeg, A. 2000. Environmental tracers in subsurface hydrology, 1st edition. Kluwer Academic Publishers: 529 p. New York. http://dx.doi.org/10.1007/978-1-4615-4557-6

Cooper, M.A.; Addison, F.T.; Alvarez, R.; Coral, M.; Graham, R.H.; Hayward, A.B.; Howe, S.; Martinez, J.; Naar, J.; Peñas, R.; Pulham, A.J.; Taborda, A. 1995. Basin development and tectonic history of the Llanos Basin, Eastern Cordillera, and Middle Magdalena Valley, Colombia. AAPG Bulletin 79 (10): 1421-1442. https://doi.org/10.1306/7834D9F4-1721-11D7-8645000102C1865D

Craig, H. 1961. Isotopic variations in meteoric waters. Science 133 (3465): 1702-1703. https://doi.org/10.1126/science.133.3465.1702

Dansgaard, W. 1964. Stable isotopes in precipitation. Tellus 16 (4): 436-468. https://doi.org/10.3402/tellusa.v16i4.8993

Davis, E.; Elderfield, H. 2004. Hydrogeology of the Oceanic Lithosphere, 1st edition. Cambridge University Press: 726 p. Cambridge.

Dengo, C.; Covey, M. 1993. Structure of the Eastern Cordillera of Colombia: implications for trap styles and regional tectonics. AAPG Bulletin 77 (8): 1315-1337. https://doi.org/10.1306/BDFF8E7A-1718-11D7-8645000102C1865D

DePaolo, D.J.; Ingram, B.L. 1985. High-resolution stratigraphy with strontium isotopes. Science 227 (4689): 938-941. https://doi.org/10.1126/science.227.4689.938

Dickin, A.P. 2018. Radiogenic isotope geology, 3rd edition. Cambridge University Press: 482 p. Cambridge. https://doi.org/10.1017/9781316163009

Drever, J.I. 1982. The preparation of oriented clay mineral specimens for X-ray diffraction analysis. *In* The Preparation and Study of Clay Mineral Standards (Drever, J.; editor), Boulder, CO: Clay Minerals Society: 38-49. Boulder, CO.

Drever, J.I. 1997. The geochemistry of natural waters: surface and groundwater environments, 3rd edition. Prentice Hall: 436 p. New Jersey.

Farrell, J.; Clemens, S.; Peter, L. 1995. Improved chronostratigraphic reference curve of late Neogene seawater $^{87}Sr/^{86}Sr$. Geology 23 (5): 403-406. https://doi.org/10.1130/0091-7613(1995)023%3C0403:ICRCOL%3E2.3.CO;2

Fetter, C.W. 1994. Applied Hydrogeology, 4th edition. Prentice-Hall Inc.: 615 p. New Jersey.

Fitts, C.R. 2002. Groundwater science, 1st edition. Academic Press: 467 p. London.

Garcia, M.; Mier, R.; Cruz, L.; Vásquez, M. 2009. Evaluación del potencial hidrocarburifero de las cuencas colombianas. Grupo de Investigación en Geología de Hidrocarburos y Carbones, Universidad Industrial de Santander. Informe ejecutivo: 219 p.

García, M.; Vargas, O.; Santos, C.; Bernal., F.; Olaya, G.; Rosero, M.; Ceballos, J.; Gonzalez, J.; Alfonso, N.; Garzón, C.; Campillo, A.K.; Onofre, C.H.; Arévalo, D.; Campuzano, C.; Rodríguez, C.; González, J.E.; Guzmán, A.; Parada, G.; Zárate, E.; Tetay, C.; Orjuela, L.C.; Cárdenas, O.; Díaz, D.P.; Castañeda, C.A.; Beltrán, M.; Montoya, J.J.; Contreras, C.; Caicedo, F.M.; Aguirre, S. 2014. Estudio Nacional del Agua 2014. IDEAM: 493 p. Bogotá.

Gibbs, R.J. 1970. Mechanisms controlling world water chemistry. Science 170 (3962): 1088-1090. https://doi.org/10.1126/science.170.3962.1088

Gómez, E.; Jordan, T.; Allmendinger, R.; Hegarty, K.; Kelley, S.; Heizler, M. 2003. Controls on architecture of the late Cretaceous to Cenozoic southern middle Magdalena Valley basin, Colombia. Geological Society of America Bulletin 115 (2): 131-147. https://doi.org/10.1130/0016-7606(2003)115<0131:COAOTL>2.0.CO;2

Gómez, E.; Jordan, T.; Allmendinger, R.; Cardozo, N. 2005a. Development of the Colombian foreland-basin system as a consequence of diachronous exhumation of the northern Andes. Geological Society of America Bulletin 117 (9-10): 1272-1292. https://doi.org/10.1130/B25456.1

Gómez, E.; Jordan, T.; Allmendinger, R.; Hegarty, K.; Kelley, S. 2005b. Syntectonic Cenozoic sedimentation in the northern middle Magdalena Valley Basin of Colombia and implications for exhumation of the Northern Andes. Geological Society of America Bulletin 117 (5-6): 547-569. https://doi.org/10.1130/B25454.1

Gutiérrez, M.; Castro, R.; Corredor, L.; Fernández, F.; Zapata, J.; Jimenez, J.; Reyes, J.; Rojas, D.; Jimenez. R.; Acosta, T.; Dueñas, E.; Solorzano, P.; Mayorga, H.; Llanos, S.; Quintero, H.; García, H. 2024. *In* SPE Improved Oil Recovery Conference. Tulsa. https://doi.org/10.2118/218173-MS

Hem, J. 1989. Study and interpretation of the chemical characteristics of natural water, 3rd edition. U.S. Geological Survey, Water-Supply Paper 2254: 272 p. Alexandria.

Hincapié, G.; Ríos, M.; Huguett, A.; Cardona, A. 2004. Atlas de aguas subterraneas de Colombia en escala 1:500.000: 987 p. Bogotá.

Hitchon, B.; Perkins, E.; Gunter, W. 1999. Introduction to Ground Water Geochemistry, Geoscience Publishing, 310 p. Sherwood Park.

Lundegard, P.; Kharaka, Y. 1994. Distribution and occurrence of organic acids in subsurface waters. *In* Organic acids in geological processes (Pittman, E.D.; Lewan, M.D.; editors). Springer: 40-69. Heidelberg. https://doi.org/10.1007/978-3-642-78356-2_3

Malagón, J. 2017. Análisis Hidrogeoquímico Multivariado del Agua Subterránea del Sistema Acuífero del Valle Medio del Magdalena-Colombia. M.Sc. Thesis. Universidad Nacional de Colombia: 85 p. Bogota

Malagón, J.; Piña, A.; Argüello, S.; Donado, L. 2021. Análisis hidrogeoquímico-multivariado del agua subterránea del sistema acuífero del Valle Medio del Magdalena, Colombia: estudio a escala regional. Boletín de la Sociedad Geológica Mexicana 73 (3): A070421. https://doi.org/10.18268/bsgm2021v73n3a070421

Mearns, E.W.; McBride, J.J. 1999. Hydrocarbon filling history and reservoir continuity of oil fields evaluated using $^{87}Sr/^{86}Sr$ isotope ratio variations in formation water, with examples from the North Sea. Petroleum Geoscience 5: 17-27. https://doi.org/10.1144/petgeo.5.1.17

Mejía, O. 2008. El recurso hídrico en la jurisdicción de Corantioquia (1995-2007). Corantioqia: 206 p. Medellín.

Mifflin, M. 1988. Region 5, Great Basin. *In* Hydrology (Back, W.; Rosenshein, J.S.; Seaber, P.R.; editors). Geological Society of North America: 69-78. Washington D.C. https://doi.org/10.1130/DNAG-GNA-O2.69

Morales, L.G.; Podesta, D.; Hatfield, W.; Tanner, H.H.; Jones, S.H.; Barker, M.H.S.; O'Donoghue, D.J.; Mohler, C.E.; Dubois, E.P.; Jacobs, C.; Goss, C.R. 1958. General geology and oil occurrences of Middle Magdalena Valley, Colombia: South America. *In* Habitat of oil symposium (Weeks, L.G.; editor). American Association of Petroleum Geologists: 641-695. Tulsa.

Pacheco-Mendoza, J.; Tesón-Del Hoyo, E.; García-González, M.; Mora, A.; Ketcham, R. 2024. Timing of hydrocarbon charge in the Axial Zone of the Eastern Cordillera, Colombia. Petroleum Geoscience 30 (3): petgeo2023-114. https://doi.org/10.1144/petgeo2023-114

Palmera, T. 2023. Efectos de la interacción de los hidrocarburos sobre la diagénesis en reservorios de arenas siliciclásticas. Ejemplo Formación Mugrosa, cuenca Valle Medio del Magdalena (VMM), Colombia. Ph.D. Thesis. Universidad EAFIT: 180 p. Medellín.

Pastor-Chacón, A.; Aguilera, R.; Triana, J.; Paez-Reyes, M.; Cantisano, M.; Bravo, L.; Gamba, N.; Niño, M.; Delgado, A.; Mendoza, G.; Rodríguez, J.D.; Romero-Ballén, O.; Ruiz, M.C.; Buitrago, H.; Fuenzalida, H. 2023. Sweet spot areas for shale oil and shale gas plays in the Upper Cretaceous rocks of the Middle Magdalena Valley, Colombia: insights from basin modeling. Frontiers in Earth Science 11: 1146126. https://doi.org/10.3389/feart.2023.1146126

Piña, A.; Donado, L.; Silva, L.; Pescador, J. 2022. Seasonal and deep groundwater-surface water interactions in the tropical Middle Magdalena River basin of Colombia. Hydrological Processes 36 (11): e14764. https://doi.org/10.1002/hyp.14764

Piper, A. 1944. A graphic procedure in the geochemical interpretation of water-analyses. Eos, Transactions American Geophysical Union 25 (6): 914-928. https://doi.org/10.1029/TR025i006p00914

Ramón, J.; Dzou, L.; Giraldo, B. 1997. Geochemical evaluation of the middle Magdalena Basin, Colombia. CT&F-Ciencia, Tecnologia & Futuro 1 (3): 47-66. https://doi.org/10.29047/01225383.587

Ramón, J.; Dzou, L.; Hughes, W.; Holba, A. 2001. Evolution of the Cretaceous organic facies in Colombia: implications for oil composition. Journal of South American Earth Sciences 14 (1): 31-50. https://doi.org/10.1016/S0895-9811(01)00010-4

Rangel, A.; Giraldo, B.; Magoon, L.; Sarmiento, L.; Bartels, H.; Mora, C.; Cordoba, F.; Luna, O.; Reyes, J. 1996. Oil potential of the Cretacic megasequence and associated oil families in the Middle Magdalena Valley, Colombia. *In* Congreso Latinoamericano de Geoquímica Orgánica, No. 5, Memorias: 105. Cancún.

Rangel, A.; Parra, P.; Niño, C. 2000. The La Luna formation: chemostratigraphy and organic facies in the Middle Magdalena Basin. Organic Geochemistry 31 (12): 1267-1284. https://doi.org/10.1016/S0146-6380(00)00127-3

Rivera, M.; Montes, L.; Castillo, L. 2025. Pore pressure estimation of the calcareous formations in the Middle Magdalena Valley Basin, Colombia. Acta Geophysica 73: 1349-1361. https://doi.org/10.1007/s11600-024-01357-9

Sarmiento, L.F. 2011. Volume 11, Middle Magdalena Basin. *In* Petroleum Geology of Colombia (Cediel, F.; Ojeda, G.Y.; editors). Universidad EAFIT: 193 p. Medellín.

Schiavo, M.; Hauser, S.; Povinec, P. 2009. Stable isotopes of water as a tool to study groundwater-seawater interactions in coastal south-eastern Sicily. Journal of Hydrology 364 (1-2): 40-49. https://doi.org/10.1016/j.jhydrol.2008.10.005

Simpson, G. 2024. Model constraints on infiltration of surface-derived fluids deep into the brittle crust. Geophysical Journal International 239 (1): 646-661. https://doi.org/10.1093/gji/ggae295

Surdam, R.C.; Jiao, Z.S.; MacGowan, D.B. 1993. Redox reactions involving hydrocarbons and mineral oxidants: A mechanism for significant porosity enhancement in sandstones. AAPG Bulletin 77 (9): 1509-1518. https://doi.org/10.1306/BDFF8ED4-1718-11D7-8645000102C1865D

Thompson-Butler, W.; Peters, K.; Magoon, L.; Scheirer, A.; Moldowan, J.; Blanco, V.; Gonzalez, R.; Graham, S.; Zumberge, J.; Wavrek, D. 2019. Identification of genetically distinct petroleum tribes in the Middle Magdalena Valley, Colombia. AAPG Bulletin 103 (12): 3003-3034. https://doi.org/10.1306/04101918107

Tissot, P.; Welte, D. 1984. Petroleum formation and occurrence, 2nd edition. Springer-Verlag: 702 p. Heidelberg.

Tostado, M. 2010. Desarrollo hidrogeoquímico de la Cuenca San Miguel, Baja California. M.Sc. Thesis. Centro de Investigacion Cientifica y de Educación Superior de Ensenada: 99 p. Ensenada.

Vargas, N.; Campillo, A.; García, M.; Jaramillo, O. 2013. Aguas subterráneas en Colombia una visión general. Instituto de Hidrología, Meteorología y Estudios Ambientales (IDEAM): 284 p. Bogotá.

Veizer, J. 1989. Strontium isotopes in seawater through time. Annual Review of Earth and Planetary Sciences 17: 141-167. https://doi.org/10.1146/annurev.ea.17.050189.001041

Manuscript received: January 17, 2024; revised/accepted: August 29, 2025; available online: September 05, 2025.